Portfolio insurance under rough volatility and Volterra processes

JEAN-LOUP DUPRET

LIDAM-ISBA, UCLouvain, Voie du Roman Pays 20
Louvain-La-Neuve, 1348, Belgium
jean-loup.dupret@uclouvain.be

DONATIEN HAINAUT

LIDAM-ISBA, UCLouvain, Voie du Roman Pays 20
Louvain-La-Neuve, 1348, Belgium
donatien.hainaut@uclouvain.be

Affine Volterra processes have gained more and more interest in recent years. In particular, this class of processes generalizes the classical Heston model and the more recent rough Heston model. The aim of this work is hence to revisit and generalize the constant proportion portfolio insurance (CPPI) under affine Volterra processes. Indeed, existing simulation-based methods for CPPI do not apply easily to this class of processes. We instead propose an approach based on the characteristic function of the log-cushion which appears to be more consistent, stable and particularly efficient in the case of affine Volterra processes compared with the existing simulation techniques. Using such approach, we describe in this paper several properties of CPPI which naturally result from the form of the log-cushion's characteristic function under affine Volterra processes. This allows to consider more realistic dynamics for the underlying risky asset in the context of CPPI and hence build portfolio strategies that are more consistent with financial data. In particular, we address the case of the rough Heston model, known to be extremely consistent with past data of volatility. By providing a new estimation procedure for its parameters based on the PMCMC algorithm, we manage to study more accurately the true properties of such CPPI strategy and to better handle the risk associated with it.

Keywords: Portfolio insurance ; CPPI ; Volterra process ; Rough volatility ; Particle Monte Carlo Markov Chain.

1. Introduction

The constant proportion portfolio insurance (CPPI) is a dynamic strategy of investment that yields a super-linear participation in future asset returns while retaining a security guarantee on a part of the invested capital (called the floor). Under the assumption of frictionless trading, this strategy therefore protects a portfolio of stocks against the downside risk but still allows for an upside potential. Basically, the CPPI method consists in maintaining the risk exposure equal to a constant multiple of the excess of wealth over a floor. The CPPI was introduced for a portfolio of bonds by Perold & Sharpe (1988) and revisited by Black & Jones (1987) for equities. A first stream of literature extensively studies the theoretical properties of continuous-time CPPI strategies. A comparison of OBPI (option-based portfolio insurance) and CPPI is provided in Bertrand & Prigent (2001) under the classical

Black and Scholes (B&S) framework and under the assumption of frictionless trading. This first set of research also deals with the effects of jump processes, stochastic volatility models, regime switching models and gap risk on the CPPI method, cfr Cont & Tankov (2009), Prigent & Bertrand (2003), Hainaut (2011), Balder *et al.* (2009) and references therein. The second stream of literature focuses on solving an optimization problem that arises when we assume investors maximize their end-of-period expected utility. In this setting, the optimality of the CPPI strategy depends on the risk profile of the investor, which has been thoroughly studied in Kingston (1989), Grossman & Vila (1992), Branger *et al.* (2010), Bertrand & Prigent (2019). Finally, the third stream tries to identify problems with the design of CPPI strategies and then proposes modifications to mitigate them. We refer to Pain & Rand (2008) for a summary of the different variations of CPPI proposed in the literature.

Our contribution lies within the framework of the first stream of literature. In this paper, we derive a methodology based on the characteristic function of the log-cushion, which enables to derive and study the properties of continuous-time CPPI with frictionless trading under the very general class of affine Volterra processes, as defined in Abi Jaber *et al.* (2019). In fact, we show that the characteristic function of the log-cushion for affine Volterra processes is obtained in quasi-closed form, which then allows to easily and efficiently compute the moments, the density as well as several risk-measures for the CPPI value at maturity. Our approach is therefore not restricted to the study of CPPI properties under a particular model as already done in the literature but extends directly and easily to a wide class of models, allowing to take into account different market behaviors and more realistic dynamics for the underlying risky asset in the context of CPPI. Moreover, using the log-cushion's characteristic function instead of the existing simulation-based techniques allows to derive far more rapidly and more accurately the desired portfolio properties.

In particular, we will focus our analysis on CPPI properties under the rough Heston model, which is an important member among the class of affine Volterra processes (based on a power-law kernel), enjoying growing popularity among practitioners and academicians. Indeed, the rough Heston model of El Euch & Rosenbaum (2019) is a highly tractable implementation of rough volatility models which has been shown to be remarkably consistent with financial time series data, as initially explained in Gatheral *et al.* (2018). The rough Heston model therefore allows to better assess the true properties of the CPPI strategy compared with other dynamics for the underlying asset. More precisely, we will demonstrate that thanks to its rough variance process, the rough Heston model will lead to a more accurate assessment of the risk of the CPPI strategy by providing a better modeling of the left tail of the portfolio distribution. Indeed, as explained in Paulot & Lacroze (2009), this left tail must be computed with great precision since it plays an important role in the

riskiness of such CPPI strategy. However, the non-Markovian nature of the variance process under the rough Heston model requires to deviate from the classical stochastic volatility approach for CPPI described in Prigent & Bertrand (2003) and to work with the characteristic function of the log-cushion instead. Moreover, the analysis of CPPI properties (performance, density and risk measures) will be carried out for the classical Heston model as well, which also belongs to the class of affine Volterra processes and for which well-established simulation techniques exist. Finally, we will compare the obtained results with the B&S model, which has already been extensively studied in the context of CPPI. In the last practical part of the paper, we will show how to introduce gap risk and transaction costs in such CPPI strategy based on affine Volterra processes and hence go beyond the assumption of frictionless/continuous trading.

At last, we contribute with this work to provide a full econometric estimation of the rough Heston's parameters based on the time series of observed log-returns using the Particle Monte-Carlo Markov Chain algorithm. So far, this rough Heston model has only been calibrated in the literature based on risk-neutral option quotes observed on the market and we now propose a new estimation procedure for deriving these parameters directly and efficiently under the real-world probability measure, which is necessary in the case of portfolio insurance. This way, we will also show that the rough Heston model provides a better statistical fit of past log-return data compared with the Heston and B&S models.

2. Model setup under rough volatility

As mentioned above, the CPPI strategy consists in maintaining the risk exposure equal to a constant multiple m of the excess of wealth over a floor F. This way, the value of the portfolio P is above the floor F at any time t in the considered period of time $[0, T]$. The value of the floor thus gives the dynamical insured amount and is assumed to evolve at a constant interest rate r following

$$dF_t = F_t\, r\, dt\,.$$

Note that a more complex dynamic could be chosen for modeling the interest rates but this choice does not impact the conclusions of our work. Obviously, the initial floor F_0 is less than the initial portfolio value P_0 and is equal to $F_0 = e^{-rT}G$, where G is the guaranteed amount at maturity. The difference $P_0 - F_0$ is called the cushion, denoted by C_0. Its value C_t at any time t in $[0, T]$ is given by

$$C_t = P_t - F_t\,.$$

Now denote the exposure E_t, which is the total amount invested in the risky asset S_t. The standard CPPI method consists of letting $E_t = mC_t$ where m is the constant multiple. In order to have a convex payoff in the underlying, we impose $m > 1$. From Bertrand & Prigent (2016), we have that m is an exogenous parameter

chosen by the portfolio manager. A first alternative is to choose m as the inverse of the maximal negative daily return anticipated by the fund manager. For example, if the manager expects that the worst daily return will be -25% over $[0, T]$, then the upper bound on the multiple m such that the value of the fund P_t remains above the floor F_t for all time $t \in [0, T]$ is given by 4. A more accurate alternative is to choose m according to the occurrence probabilities of extreme events in the risky asset such as described in Bertrand & Prigent (2016). We will apply their methodology in Section 6 to provide an upper bound of the multiple m based on a dataset of S&P500 daily log-returns.

Moreover, we consider in this paper a continuous-time CPPI strategy and we assume in a first step continuous/frictionless trading over the whole investment horizon $[0, T]$. In the last section, we will then briefly discuss the possible ways of taking into account gap risk, borrowing constraints and transaction costs by restricting trading on a discrete time grid.

We also assume in the sequel that the risky asset S_t is a diffusion process such that

$$dS_t = S_t \left(\mu \, dt + \sqrt{V_t} \, dW_t \right), \tag{2.1}$$

where W_t is a standard Brownian motion defined on a probability space $(\Omega, \mathcal{F}, \mathbb{P})$ with a right-continuous filtration $(\mathcal{F}_t)_{t \geq 0}$. The cornerstone of this section is to consider that the variance process V_t exhibits a rough behavior. Indeed, in their groundbreaking paper, Gatheral *et al.* (2018) show that for a very wide range of assets, historical volatility time series exhibit a behavior that is much rougher than that of a Brownian motion (as implied by standard stochastic volatility models). More precisely, they emphasize that volatility dynamics based on fractional Brownian motions with a Hurst exponent in $\left(0, \frac{1}{2}\right)$ are extremely consistent with the historical volatility process of major indices. Such condition on the Hurst index aims to generate rough sample paths and to introduce short-range dependence in the volatility process, as explained in Gatheral *et al.* (2018). On the contrary to long-memory volatility models ($H > 1/2$), this rough behavior of volatility allows to perfectly reproduce at any time scales a lot of statistical properties of the past volatility time series, as confirmed in many other studies, such as in Bennedsen *et al.* (2016). Furthermore, Gatheral *et al.* (2018) find that classical statistical procedures aiming at detecting volatility persistence tend to conclude the presence of long memory in data generated from their rough volatility model. This allows these authors to explain and understand why long memory of volatility has been widely accepted as a stylized fact until now. This recent change of paradigm towards rough volatility, both by academicians and practitioners, allows to study more accurately the true properties of CPPI strategies. Indeed, such comparisons with other portfolio insurance techniques have been mainly limited so far to the B&S case or to classical stochastic volatility models based on Brownian motions. We will show in this paper

the impact of taking into account rough volatility on CPPI properties by considering the rough Heston model of El Euch *et al.* (2018) and we will explain why it provides a better modeling of the risk associated with the CPPI strategy. This rough Heston model is in fact an extension of the the classical Heston model where El Euch *et al.* (2018) introduce the power-law kernel $(t-u)^{H-1/2}$ in the Heston variance process V_t in order to allow for a rough behavior of V_t in a Heston-type model. They hence find the following variance process under the rough Heston model

$$V_t = V_0 + \frac{1}{\Gamma(H+1/2)} \int_0^t \frac{\lambda\,(\theta - V_u)}{(t-u)^{1/2-H}} du + \frac{\nu}{\Gamma(H+1/2)} \int_0^t \frac{\sqrt{V_u}}{(t-u)^{1/2-H}}\, d\widehat{W}_u\,, \tag{2.2}$$

where λ is the speed of mean reversion of the variance process towards the level θ and where ν is the volatility of variance parameter. $\widehat{W}_t$ is again a standard Brownian motion defined on $(\Omega, \mathcal{F}, \mathbb{P})$ such that $\langle W, \widehat{W}\rangle_t = \rho\, t$ with a constant correlation ρ. When $H = 1/2$, we can verify that we indeed recover the classical Heston model. It can also be shown that the trajectories of the variance itself under the rough Heston are almost surely Hölder-continuous of order $H - \varepsilon$, for any $\varepsilon > 0$, leading to a rough behavior of the variance process with short-range memory when $H < 1/2$ and smoother trajectories with long-range dependence when $H > 1/2$. These authors also provide a microstructure foundation of such model as shown in El Euch & Rosenbaum (2019).

We now define the forward variance curve $\xi_s(t) := \mathbb{E}[V_t|\mathcal{F}_s]$, $t \geq s$. We can easily recover V_s from $\xi_s(t)$ as $V_s = \lim_{t\to s} \xi_s(t)$. Following Bergomi & Guyon (2012), forward variance models are models that can be written as a function of this curve $\xi_s(t)$. As shown in El Euch *et al.* (2018), this is the case of the rough Heston model (2.2). More precisely, we have the following forward variance curve dynamic for this rough Heston model

$$d\xi_s(t) = \nu(t-s)^{\alpha-1} E_{\alpha,\alpha}(-\lambda(t-s)^\alpha)\sqrt{V_s}\, d\widehat{W}_s\,. \tag{2.3}$$

where $\alpha = H + 1/2$ and $E_{\alpha,\beta}(z)$ denotes the generalized Mittag-Leffler function defined by

$$E_{\alpha,\beta}(z) = \sum_{k=0}^{\infty} \frac{z^k}{\Gamma(\alpha k + \beta)}\,.$$

Let now $\eta_s(t) = \sqrt{V_s}\,\kappa(t-s)$ where $\kappa(t-s) = \nu(t-s)^{\alpha-1} E_{\alpha,\alpha}(-\lambda(t-s)^\alpha)$, we can then rewrite (2.3) as

$$d\xi_s(t) = \eta_s(t) d\widehat{W}_s\,. \tag{2.4}$$

This writing will be useful in the sequel to ease notations. Note that $\eta_s(t)$ satisfies the Assumption 2.1. of Gatheral & Keller-Ressel (2019) as shown in the proof of Appendix 10.2 and that $\kappa(t-s)$ is a decreasing L_2-kernel, which is necessary in the following of the paper to define the characteristic function of the log-cushion.

Moreover, it is shown in El Euch *et al.* (2018) that the initial forward variance curve at time $s = 0$ in the rough Heston model is given by

$$\xi_0(t) = V_0 + (\theta - V_0)\,\frac{\lambda}{\nu}\int_0^t \kappa(s)ds \tag{2.5}$$

3. CPPI in the rough Heston model

Under the assumption of frictionless trading for CPPI, we can first consider the stochastic volatility case of Prigent & Bertrand (2003) where the volatility σ_t of the underlying risky asset S_t is stochastic. They first show that the cushion value at any time t is

$$C_t = C_0 \exp\left\{(r + m(\mu - r))\,t - \frac{1}{2}m^2\int_0^t V_s\,ds + m\int_0^t \sqrt{V_s}\,dW_s\right\}. \tag{3.1}$$

Then, from

$$S_t^m = S_0^m \exp\left\{m\left(\mu\,t - \frac{1}{2}\int_0^t V_s\,ds\right) + m\int_0^t \sqrt{V_s}\,dW_s\right\}, \tag{3.2}$$

Prigent & Bertrand (2003) find that :

$$C_t = S_t^m \alpha_t\,, \tag{3.3}$$

with $\alpha_t = \left(\frac{C_0}{S_0^m}\right)\exp\{\beta_t\,t\}$ and $\beta_t = -(m-1)r - \frac{1}{2}\left(m^2 - m\right)\frac{1}{t}\int_0^t V_s\,ds\,.$

Finally, since the CPPI fund is the sum of the cushion and the floor, we get that $P_t = F_t + S_t^m\alpha_t$. On the contrary to the B&S framework, we no longer have that the parameter α_t is a constant but a random variable instead. Moreover, the portfolio value P_t now depends on the whole path of the variance process $\int_0^t V_s ds$ and hence, the short-memory of the rough-Heston variance process with $H < 1/2$ will have an impact on P_t. However, expressions (3.2) and (3.3) will not be useful in our case, *i.e.* when the variance process exhibits a rough behavior as in equation (2.2). Indeed, as explained in El Euch *et al.* (2018), the rough Heston model is non-Markovian with respect to the current variance state V_s, which makes the quantity $\int_0^t V_s\,ds$ hard to compute and to obtain from Monte-Carlo simulations and even from more advanced numerical schemes such as the Hybrid scheme of Bennedsen *et al.* (2017). However, Gatheral & Keller-Ressel (2019) show that the rough Heston is Markovian in the forward variance curve $\xi_s(t)$. Indeed, given the state vector $\xi_s(t)$, the dynamics of the model are well-determined. Hence, we will now capitalize on this Markov property with respect to $\xi_s(t)$ in order to compute more precisely and efficiently the value of the CPPI portfolio at any time t. Denoting $X_t = \log C_t$, it is useful to rewrite equation (3.1) as

$$dX_t = (r + m(\mu - r))\,dt - \frac{1}{2}m^2\,V_t\,dt + m\sqrt{V_t}\,dW_t = (r + m(\mu - r))\,dt + dY_t\,, \tag{3.4}$$

where

$$dY_t = -\frac{1}{2}m^2\, V_t\, dt + m\sqrt{V_t}\, dW_t. \tag{3.5}$$

We now want to obtain the characteristic function of the forward variance model (Y, ξ), *i.e.* of the process Y together with the family of processes $(\xi_s(t))_{t\geq s}$. From *Theorem 2.6.* of Gatheral & Keller-Ressel (2019) and from the dynamic of $\xi_s(t)$ given in equation (2.4), we have that that our forward variance model (Y, ξ) has an affine cumulant-generating function (CGF) in the sense that its CGF is of the form

$$\log \mathbb{E}\left[e^{u(Y_T - Y_s)}|\mathcal{F}_s\right] = \int_s^T g(T-r, u)\xi_s(r)dr\,, \tag{3.6}$$

for all $u \in [0,1],\ 0 \leq s \leq T$ and where $g(\cdot, u)$ is $\mathbb{R}_-$-valued and continuous on $[0,T]$ for all $T > 0$ and $u \in [0,1]$. This leads to the following theorem :

Theorem 3.1. *The function $g(\cdot, u) : \mathbb{R}_+ \to \mathbb{R}_-$ is the unique global continuous solution of the fractional Riccati equation*[a] *:*

$$g(t,u) = R_v\left(m, u, \int_0^t \kappa(t-r)g(r,u)dr\right) = R_v\left(m, u, (\kappa \star g)(t,u)\right), \tag{3.7}$$

where

$$R_v(m,u,w) = \frac{1}{2}m^2(u^2-u) + m\rho u w + \frac{1}{2}w^2\,. \tag{3.8}$$

Proof. Cfr Appendix 10.2. □

We now show how to determine the function $g(\cdot, u)$ in the case of the CPPI under the rough Heston model (2.2). First let's denote

$$\psi(t,u) = \frac{1}{\nu}(\kappa \star g)(t,u) = \int_0^t (t-s)^{\alpha-1} E_{\alpha,\alpha}\left(-\lambda(t-s)\right) g(s,u)ds\,.$$

Thanks to Lemma A.2 of El Euch & Rosenbaum (2019), we find

$$D^\alpha \psi(t,u) + \lambda\, \psi(t,u) = g(t,u)\,.$$

Then, using relations (3.7) and (3.8) with the fact that $(\kappa \star g)(t,u) = \nu\, \psi(t,u)$, we obtain

$$D^\alpha \psi(t,u) = \frac{1}{2}m^2(u^2-u) + (m\,\rho\, u\, \nu - \lambda)\, \psi(t,u) + \frac{1}{2}\nu^2\, \psi(t,u)^2\,. \tag{3.9}$$

Finally, we can transform the affine CGF (3.6) into a characteristic function by imposing $u = iz$. Therefore, we obtain the following characteristic function in forward-variance form of (Y, ξ) for the rough Heston, conditionally on the initial state (Y_s, ξ_s) :

$$\Phi_s^Y(T,z) = \mathbb{E}\left[e^{izY_T}\,\middle|\, Y_s, \xi_s\right] = \exp\left\{izY_s + \int_s^T D^\alpha \psi(T-r, iz)\xi_s(r)\, dr\right\}. \tag{3.10}$$

[a] The convolution operator $\star$ between two functions f, g is defined as : $(f \star g)(t) := \int_0^t f(t-r)g(r)dr$.

From equation (2.5) and Appendix 10.1 on fractional calculus, we can easily rewrite the initial characteristic function of (Y, ξ) at time $s = 0$ as

$$\Phi_0^Y(T,z) = \mathbb{E}\left[e^{izY_T} \middle| Y_0, V_0\right] = \exp\left\{izY_0 + \int_0^T \psi(T-r, iz)\left(\lambda\theta + \frac{V_0\, r^{-\alpha}}{\Gamma(1-\alpha)}\right) dr\right\}. \tag{3.11}$$

The characteristic function of the log-cushion in forward variance form (X, ξ) at time $s = 0$ for the rough Heston model directly follows from (3.11) :

$$\Phi_s^X(T,z) = \mathbb{E}\left[e^{izX_T} \middle| X_0, V_0\right] = \exp\left\{iz\left(X_0 + (r + m(\mu - r))\, T\right) + \int_0^T \psi(T-r, iz)\left(\lambda\theta + \frac{V_0\, r^{-\alpha}}{\Gamma(1-\alpha)}\right) dr\right\}. \tag{3.12}$$

The key issue we tackle in this paper is to propose the most appropriate dynamic of the underlying risky asset under $\mathbb{P}$ using statistical methods on financial data such as to obtain the true properties of CPPI strategy. We are therefore interested in the dynamic of the portfolio under the real probability measure $\mathbb{P}$ and we hence need to estimate the parameters $(\alpha, \mu, \lambda, \theta, \nu, \rho)$ based on the observed time series of log-returns. Moreover, having a characteristic function in quasi-closed form for the log-cushion value X_t thanks to equation (3.12), we can obtain easily and efficiently several risk measures for C_t such as the VaR and TVaR, as well as its moments of all orders. This will be discussed in the following sections.

4. Estimation of the rough Heston model

We first choose as starting date $t = 0$, the 31^{st} of July 2021. Since we decide throughout this paper to consider a fixed investment horizon of $T = 1$ year for the CPPI strategy, we use the U.S. swap rate for this maturity equal to $r = 0.2546\%$. Then, in order to estimate the parameters of our model, we consider daily time series of log-returns from January 2017 to July 2021 for the S&P500 making a total of 1141 data points. In the literature so far, calibration of the rough Heston model has been exclusively done based on risk neutral option quotes such as in El Euch *et al.* (2019) or Dupret *et al.* (2021). We now introduce a new approach for providing a full econometric estimation of the rough Heston's parameters under the real probability measure $\mathbb{P}$, which is based on the Particle Markov Chain Monte Carlo (PMCMC) procedure of Andrieu *et al.* (2010). This algorithm is built from a sequential Monte-Carlo filter that we now describe.

4.1. *Filtering*

This section introduces the filtering technique, also called sequential Monte-Carlo (SMC) filter, that is used to determine the most likely evolution of the hidden vari-

ance process V_t. There is a considerable literature on the development of simulation-based methods to perform filtering of nonlinear Gaussian models. Leading contributions are reviewed by Doucet *et al.* (2001). This SMC will be combined in the sequel with a Monte-Carlo Markov Chain to estimate the parameters of the rough Heston model but for the moment, we assume that its parameters are known. We consider a sample of discrete observations of log-returns $R_t = \ln \frac{S_{t+\Delta}}{S_t}$ where Δ is the time step between two observations. The sample is denoted by $r = \{r_1, r_2, \dots, r_n\}$ where $n = T/\Delta$. We denote v_j and r_j the realizations of V_{t_j} and R_{t_j} for $j = 1, \dots, n$ with $t_n = T$. The dynamic of log-returns is approached by applying Itô Lemma on equation (2.1) and then discretizing the obtained equation, which gives

$$R_{j+1} = \left(\mu - \frac{V_j}{2}\right)\Delta + \sqrt{V_j}\,\Delta W_{j+1}\,.$$

The increment ΔW_j can be rewritten as $\Delta W_j = \sqrt{1-\rho^2}\,\Delta W_j^1 + \rho\,\Delta W_j^2$ where $\Delta W_j^1 \sim N(0, \sqrt{\Delta})$ and where $\Delta W_j^2 \sim N(0, \sqrt{\Delta})$. Therefore, we have

$$R_{j+1} = \left(\mu - \frac{V_j}{2}\right)\Delta + \sqrt{1-\rho^2}\,\sqrt{V_j}\,\Delta W_{j+1}^1 + \rho\sqrt{V_j}\,\Delta W_{j+1}^2\,. \tag{4.1}$$

The variance process (2.2) is discretized the same manner by

$$V_{j+1} = V_0 + \sum_{k=0}^{j} \frac{(t_{j+1}-t_k)^{\alpha-1}}{\Gamma(\alpha)}\lambda\,(\theta - V_k)\,\Delta + \sum_{k=0}^{j} \frac{(t_{j+1}-t_k)^{\alpha-1}}{\Gamma(\alpha)}\nu\sqrt{V_k}\,\Delta W_{k+1}^2\,. \tag{4.2}$$

In practice, we prefer to use the much more time-efficient simulation scheme of Abi Jaber (2019) for discretizing $(V_j)_{j=1,\dots,n}$. These authors managed to build the rough variance process as superposition of infinitely many factors sharing the same Brownian motion but mean-reverting at different speeds. Limiting the number of factors allows to speed up the simulation scheme while still ensuring a extremely good proximity with the true original variance process. We denote the set of parameters $\vartheta = (\alpha, \mu, \lambda, \theta, \nu, \rho)$ and as mentioned above, it is assumed to be known for the moment. The particle filter estimates the most likely sample paths of the variance process. We denote by Δw_j^2 the realizations of ΔW_j^2. The information $V_j = v_j$ and $\Delta W_j^2 = \Delta w_j^2$ is stored in a *particle*, *i.e.* a vector denoted $u_j = \left(v_k,\, \Delta w_k^2\right)_{k=1:j}$. Contrary to classical stochastic volatility models, we now have to keep track of the whole sample path of the variance process and of the related Brownian increments in the particles from $k = 1$ to j due to the non-Markovian nature of the rough Heston model.

The visible information up to time t_j is stored in a vector $r_{1:j} = \{r_1, \dots, r_j\}$ and the density of the observation $f(r_j|u_j)$, conditionally to the information in the particle, is a Gaussian probability density function. More precisely, if we denote by $\phi(\cdot)$ the

pdf of a $N(0,1)$, we have from equation (4.1) that

$$f(r_j \,|\, u_j) = \phi\left(\frac{r_j - \left(\mu - \frac{v_{j-1}}{2}\right)\Delta - \rho\sqrt{v_{j-1}}\,\Delta w_j^2}{\sqrt{1-\rho^2}\sqrt{v_{j-1}}\,\sqrt{\Delta}}\right). \tag{4.3}$$

On the other hand, the transition density $f(u_{j+1}|u_j)$ is simulated based on equation (4.2). The initial pdf of u_0 is denoted $f(u_0)$. Then, using Bayesian arguments, one can show that the posterior distribution of u_j conditionally to the available information at t_j is equal to

$$f(u_j \,|\, r_{1:j}) = \frac{f(r_j \,|\, u_j)}{\int f(r_j \,|\, u_j) f(u_j \,|\, r_{1:j-1}) du_j} f(u_j \,|\, r_{1:j-1})\,, \tag{4.4}$$

where we predict

$$f(u_j \,|\, r_{1:j-1}) = \int f(u_j \,|\, u_{j-1}) f(u_{j-1} \,|\, r_{1:j-1})\, du_{j-1}\,. \tag{4.5}$$

The calculation of $f(u_j \,|\, r_{1:j})$ can then be performed in three steps. First, in the prediction step, we approach $f(u_j \,|\, r_{1:j-1})$ by simulations, based on relations (4.5) and (4.2). In practice, the integral in (4.5) is replaced by a Monte-Carlo simulation of N particles, denoted $u_j^{(i)}$ for $i = 1, \ldots, N$ and the density $f(u_j \,|\, r_{1:j})$ is replaced by the probability of occurrence denoted $p_j^{(i)}$ for the particle i, *i.e.* $p_j^{(i)} = P(u^{(i)} \,|\, r_{1:j})$. In the correction step, the probabilities $f(u_j \,|\, r_{1:j})$ are computed via equation (4.4). In the third step, we perform a resampling with replacement and with probabilities $p_j^{(i)}$, $i = 1, \ldots, N$ in order to keep track of the most likely sample paths of the variance process. The structure of the particle filter algorithm is presented in Appendix 10.3. Finally, the filtered variance process for the period j is computed as

$$\widehat{V_j} = \mathbb{E}(V_j \,|\, r_{i:j}) = \sum_{i=1}^{N} v_j^{(i)} p_j^{(i)}\,,$$

whereas the log-likelihood of the whole sample path is approached before resampling by the sum

$$\ln f(r \,|\, \vartheta) = \sum_{j=1}^{n} \ln\left(\sum_{i=1}^{N} p_j^{(i)} f(r_j \,|\, u_j^{(i)})\right). \tag{4.6}$$

4.2. *Econometric estimation*

We have so far considered that the set of parameters ϑ is known, which is not the case in practice. An inherent problem of particle filters is that the estimate of the likelihood is not a smooth function of parameters. Practically, the calibration of a model by maximizing the log-likelihood (*e.g.* with a gradient descent) is then uncertain. We here prefer using the PMCMC procedure which has been shown by Andrieu *et al.* (2010) and Johannes & Polson (2010) to be highly efficient for such financial estimation of stochastic volatility models. We now denote the set

of unknown parameters by $\Theta = (\alpha, \mu, \lambda, \theta, \nu, \rho)$. We here again adopt a Bayesian approach and Θ is a multivariate random variable with realizations ϑ and with state space χ. The parameters posterior distribution, based on the observed sample $r = \{r_1, \cdots, r_n\}$ is

$$f(\vartheta \,|\, r) = \frac{f(\vartheta) f(r \,|\, \vartheta)}{\int_\chi f(\vartheta') f(r \,|\, \vartheta') \, d\vartheta'} \,, \tag{4.7}$$

where $f(\vartheta)$ and $f(r \,|\, \vartheta)$ denotes respectively the parameter prior distribution and the likelihood of the data. The density $f(\vartheta \,|\, r)$ is built by the PMCMC method. It generates samples from $f(\vartheta \,|\, r)$ by creating a Markov chain with the same distribution as the parameters posterior one. Once that the Markov chain has reached stationarity after a transient phase, called *burn-in* period, samples from the posterior distribution are simulated. Standard MCMC algorithm requires a pointwise estimate of $f(r \,|\, \vartheta)$, which is not available in our model. Instead, $f(r \,|\, \vartheta)$ is approached by its estimate (4.6), yield by the particle filter of the previous section.

The construction of the Markov chain consists of two steps, repeated iteratively for $k = 1, \ldots, K$. At the beginning of the $(k+1)^{th}$ iteration, we propose a candidate parameter $\vartheta^{'}$ from a proposal distribution $q(\vartheta^{'} \,|\, \vartheta_k)$ given the previous state of the Markov chain, ϑ_k. The proposal distribution must have a support that covers the target distribution. In the second step, we determine if we update the state $\vartheta^{'}$. For this purpose, the acceptance probability of the Metropolis-Hasting algorithm described in Appendix 10.3 (cfr Algorithm 2), is computed as follows

$$\rho(\vartheta^{'}, \vartheta_k) = \min \left\{ \frac{f(\vartheta^{'} \,|\, r)}{f(\vartheta_k \,|\, r)} \frac{q(\vartheta_k \,|\, \vartheta^{'})}{q(\vartheta^{'} \,|\, \vartheta_k)}, 1 \right\}. \tag{4.8}$$

This determines the probability that we assign the candidate parameter as the next state of the Markov chain, $\vartheta^{'} \to \vartheta_{k+1}$. Intuitively, if we disregard the influence of the proposal distribution $q(\cdot, \cdot)$, a candidate is accepted if it increases the posterior likelihood $f(\vartheta^{'} \,|\, r) > f(\vartheta_k \,|\, r)$. The presence of $q(\cdot, \cdot)$ in (4.8) allows a small decrease in the posterior likelihood, such as to explore the space of parameters χ.

In numerical applications, the transition distribution $q(\vartheta^{'} \,|\, \vartheta_k)$ is assumed Gaussian, $\vartheta^{'} \sim N(\vartheta_k, \sigma_\vartheta \, I_m)$ where I_m is the identity matrix. As this distribution is symmetric, we have $q(\vartheta_k \,|\, \vartheta^{'}) = q(\vartheta^{'} \,|\, \vartheta_k)$ and the acceptance probability simplifies to

$$\rho(\vartheta^{'}, \vartheta_k) = \min \left\{ \frac{f(r \,|\, \vartheta^{'})}{f(r \,|\, \vartheta_k)} \frac{f(\vartheta^{'})}{f(\vartheta_k)}, 1 \right\}.$$

The resulting samples of parameters $\vartheta_{1:K}$ (after a burn-in period) serves next to build the empirical distribution of $f(\vartheta \,|\, r)$, which is obtained by

$$f(\vartheta \,|\, r) \approx \frac{1}{K} \sum_{k=1}^{K} \delta_{\vartheta_k}(d\vartheta) \,,$$

where $\delta_{\vartheta_k}(d\vartheta)$ are the Dirac atoms located at $\vartheta = \vartheta_k$, with equal weights. The estimate of parameters with respect to the posterior distribution is then

$$\widehat{\Theta} = \mathbb{E}(\Theta \,|\, r) = \int_{\chi} f(\vartheta \,|\, r)\, d\vartheta \approx \frac{1}{K} \sum_{k=1}^{K} \int_{\chi} \delta_{\vartheta_k}(d\vartheta) = \frac{1}{K} \sum_{k=1}^{K} \theta_k \,. \tag{4.9}$$

We now use the PMCMC algorithm to calibrate the set of parameters $\Theta = (\alpha, \mu, \lambda, \theta, \nu, \rho)$ of the rough Heston model (2.2). The standard deviation σ_ϑ of the transition distribution is set to $\sigma_\vartheta = (0.01\%, 0.01\%, 0.1\%, 0.01\%, 0.01\%, 0.1\%)$. Even if the procedure converges theoretically to parameter estimates, it is advisable to provide realistic initial parameters to improve the speed of convergence. Therefore, we impose $\vartheta_0 = (0.7, 0.05, 0.3, 0.04, 0.2, -0.7)$. The filter runs with $N = 1000$ particles and we perform $K = 20\,000$ iterations of the PMCMC procedure. Table 1 reports the rough Heston estimates with a burn-in period of 18 000 iterations. The obtained log-likelihood (4.6) is equal to 3693.66.

Table 1. Parameter estimates of the rough Heston model for the S&P500 index and standard error (std. err.) of these estimates.

	$\widehat{\alpha}$	$\widehat{\mu}$	$\widehat{\lambda}$	$\widehat{\theta}$	$\widehat{\nu}$	$\widehat{\rho}$
Estimators PMCMC	0.8504	0.1446	0.2434	0.2122	0.3528	-0.5536
PMCMC std. err.	0.0128	0.0191	0.1272	0.0239	0.0183	0.0359

We observe that the estimate of the speed of mean-reversion λ is quite volatile with a high standard error. The other parameter estimates are more reliable. The advantage of our method based on a maximum likelihood estimator (MLE) for estimating α is the nice properties associated with such MLE. It is consistent, asymptotically unbiased and of minimal variance whereas the method of moment proposed by Gatheral *et al.* (2018) only exhibits consistency. Our estimator of α is hence more accurate. However, the method of moments of these authors based on the $q-$variation of the log-volatility can be used to confirm that the roughness index of the simulated rough Heston volatility with the MLE of Table 1 is consistent with the observed regularity of the past volatility time series. Using the methodology of these authors to estimate the smoothness of the past volatility between January 2017 and July 2021, we find an estimated value of the Hurst index $\hat{H} = 0.2324$. We then simulate sample paths of our variance process V_t under the rough Heston model with $\alpha = 0.8504$ and $T = 4.5$ years (time length between January 2017 and July 2021), which gives $T \times 252 = 1142$ daily time steps. Based on these simulated sample paths, we find via the method of moments that the regularity of the corresponding volatility process is on average equal to $\hat{H} = 0.2505$, which is highly consistent with the value estimated based on the observed time series of volatility between 2017 and 2021.

5. Other models

In order to compare the rough Heston model with other models such as the Heston or B&S models in terms of CPPI properties, we need to derive the characteristic function of the log-cushion in these models. We show in this section that such log-cushion's characteristic function can be well defined analytically under affine Volterra processes and we can hence generalize the above results for this larger class of processes.

5.1. *Heston model*

First, the Heston model under the real probability measure $\mathbb{P}$ is given by

$$dS_t = S_t\,\mu\,dt + S_t\,\sqrt{V_t}\,dW_t\,, \tag{5.1}$$

$$dV_t = \lambda(\theta - V_t)\,dt + \nu\,\sqrt{V_t}\,d\widehat{W}_t\,. \tag{5.2}$$

The two Brownian motions are defined as above. We have that $V_0 = \sigma_0^2$ is the initial variance, θ is the long-run variance of V_t, λ denotes the speed of mean-reversion and ν is the volatility of variance parameter. From Bergomi & Guyon (2012), we know that the Heston model can be rewritten as a forward variance model with an affine CGF of the form of equation (3.6). Furthermore, based on *Example 2.10.* of Gatheral & Keller-Ressel (2019) and from Theorem 3.1, we obtain directly that the characteristic function of the log-cushion in the Heston model under $\mathbb{P}$ is

$$\Phi_X(T,z) = \mathbb{E}\left[e^{izX_T}\middle|\,X_0,V_0\right] = \exp\Bigg\{iz\left(X_0 + (r + m(\mu - r))\,T\right) + V_0\,\psi(T,iz) + \lambda\theta\int_0^T \psi(r,iz)dr\Bigg\}, \tag{5.3}$$

and where $\psi(\cdot,iz)$ solves a (non-fractional) Riccati equation

$$\frac{\partial}{\partial t}\psi(t,iz) = -\frac{1}{2}m^2(z^2+iz) + (miz\rho\,\nu - \lambda)\psi(t,iz) + \frac{\nu^2}{2}\,\psi(t,iz)^2\,. \tag{5.4}$$

Note that this Riccati equation is consistent with the classical ODE's initially derived for the Heston model, such as in Gatheral (2011) (with $m = 1$). We also see that the fractional derivative of the rough Heston (which conveys the short memory to the model with $H < 1/2$) is replaced by a classical time derivative in the Riccati equation.

We again apply the PMCMC procedure above with the particle filter of section 4.1 in order to estimate the parameters of the Heston model. The discretized variance process (4.2) now becomes under the Heston model

$$V_{j+1} = V_j + \lambda(\theta - V_j)\Delta + \nu\sqrt{V_j}\,\Delta W_{j+1}^2\,, \tag{5.5}$$

and we now have the particle $u_j = (v_j, \Delta w_j^2)$ so that the process $(u_j)_{j=1,\dots,n}$ is a Markov chain (note that we do not need anymore to keep track of the whole sample

path from $k = 1$ to j as in the rough Heston case). The set of unknown parameters becomes $\Theta = (\mu, \lambda, \theta, \nu, \rho)$ since we do not have to estimate the roughness parameter α, equal to 1 in the Heston model. We use the same standard deviation σ_ϑ and initial parameters ϑ_0 as in the rough Heston model (but removing their α-component). Finally, we again run the filter with $N = 1000$ particles and $K = 20\,000$ iterations and we obtain the following Table 2 with a log-likelihood equal to 3498.03.

Table 2. Parameter estimates of the Heston model for the S&P500 index and standard error of these estimates.

	$\widehat{\mu}$	$\widehat{\lambda}$	$\widehat{\theta}$	$\widehat{\nu}$	$\widehat{\rho}$
Estimators PMCMC	0.1392	0.9256	0.1435	0.4831	-0.5506
PMCMC std. err.	0.0324	0.2656	0.0532	0.0106	0.0631

We first note a lower log-likelihood compared with the rough Heston model. This significant difference of log-likelihood confirms that the rough Heston model provides a better fit from a statistical point of view. The average rate of return μ and the anti-correlation ρ are comparable between the two models. The mean reversion level θ is now lower compared to the rough Heston model while the speed of mean reversion λ is much higher. We again obtain a high standard error for the speed of mean-reversion level λ whereas the other estimates are more reliable.

5.2. *Affine Volterra processes*

The methodology described above for deriving the characteristic function of the rough Heston and Heston models can be extended to the more general class of affine Volterra processes. This class of processes is defined in Abi Jaber *et al.* (2019) by the following d-dimensional stochastic convolution equation of the form

$$Z_t = Z_0 + \int_0^t K_Z(t-s)b(Z_s)ds + \int_0^t K_Z(t-s)\sigma(Z_s)dW_s\,, \tag{5.6}$$

where W is a d-dimensional $\mathbb{P}$-Brownian motion, where K_Z is a convolution kernel such that $K_Z \in L^2_{loc}(\mathbb{R}_+, \mathbb{R}^{d\times d})$ and where the coefficients b and σ satisfy the regularity and integrability conditions studied in Abi Jaber *et al.* (2019). This class of processes is called *affine* since the coefficient $a(z) = \sigma(z)\sigma(z)^T$ (with $\sigma(z)$ positive semidefinite) and the coefficient $b(z)$ are both affine of the form

$$\begin{aligned} a(z) &= A^0 + z_1A^1 + \cdots + z_dA^d\,,\\ b(z) &= b^0 + z_1b^1 + \cdots + z_db^d\,, \end{aligned}$$

for d-dimensional symmetric matrices A^i and vectors b^i. We next introduce the $d\times d$ matrix

$$B = \begin{pmatrix} b^1 & \cdots & b^d \end{pmatrix}, \tag{5.7}$$

and for any row vector $u \in \mathbb{C}^d$, we define the row vector

$$A(u) = \left(uA^1u^T, \cdots, uA^du^T\right). \tag{5.8}$$

We then recall from the log-cushion dynamic (3.5) that

$$Y_t = Y_0 - \frac{1}{2}m^2 \int_0^t V_s \, ds + m \int_0^t \sqrt{V_s} \, dW_s \, . \tag{5.9}$$

Moreover, we now consider that the variance process V_t follows the general (one-dimensional) convolution equation given by

$$V_t = V_0 + \int_0^t K(t-s) \, (\beta + bV_s) \, ds + \int_0^t K(t-s) \left(\alpha + a\sqrt{V_s} \right) d\widehat{W}_s \, , \tag{5.10}$$

again with a constant correlation ρ such that $\langle W, \widehat{W} \rangle_t = \rho \, t$, with $\beta, b, \alpha, a \in \mathbb{R}$ and a convolution kernel $K \in L^2_{loc}(\mathbb{R}_+, \mathbb{R})$ such that :

K is strictly positive and completely monotone. There is $\gamma \in (0, 2]$ such that

$$\int_0^h K(t)^2 dt = O(h^\gamma) \text{ and } \int_0^T (K(t+h) - K(t))^2 dt = O(h^\gamma) \text{ for } T < \infty. \tag{5.11}$$

Hence, we take $d = 2$ and consider the two-dimensional process $Z = (Y, V)$. In order to have an affine Volterra process Z compatible with the given equation (5.9) of Y, we need to impose the coefficient $a(z)$ of Z to be of the form

$$A^0 = \begin{pmatrix} 0 & 0 \\ 0 & 0 \end{pmatrix} \qquad A^1 = \begin{pmatrix} 0 & 0 \\ 0 & 0 \end{pmatrix} \qquad A^2 = \begin{pmatrix} m^2 & m\rho a \\ m\rho a & a^2 \end{pmatrix} . \tag{5.12}$$

This amounts to set $\alpha = 0$ in the variance process 5.10. Otherwise, there does not exist a positive semidefinite matrix $\sigma(z)$ which is such that $a(z) = \sigma(z)\sigma(z)^T$ is affine. The coefficients $b(z)$ and the kernel of the two-dimensional affine Volterra process Z are given by

$$b^0 = \begin{pmatrix} 0 \\ \beta \end{pmatrix} \qquad B = \begin{pmatrix} 0 & -\frac{1}{2} \\ 0 & b \end{pmatrix} \qquad K_Z = \begin{pmatrix} 1 & 0 \\ 0 & K \end{pmatrix} . \tag{5.13}$$

We clearly see that the Heston model described in Section 5.1 can be retrieved by setting the kernel $K \equiv 1$ and the coefficients $a = \nu$, $\beta = \lambda\theta$ and $b = -\lambda$ in the variance process. For the rough Heston model, we need to impose a power law kernel $K(t) = t^{\alpha-1}/\Gamma(\alpha)$ for the variance process instead, which is known to satisfy the condition (5.11). We now derive from Abi Jaber *et al.* (2019) the characteristic function of the log-cushion under the two-dimensional affine Volterra process Z for general coefficients a, β, b and for general convolution kernel K.

Theorem 5.1. *Let $Z = (Y \;\; V)^T$ be a solution of (5.6) with $K_Z \in L^2(\mathbb{R}_+, \mathbb{R}^{2\times 2})$, where we assume that K satisfies (5.11) and where $A(\cdot)$ is given by (5.8). Let $u = (u_1 \;\; u_2) \in \mathbb{C}^2$ with $\mathrm{Re}\, u_1 \in [0, 1]$ and $\mathrm{Re}\, u_2 \leq 0$ and assume that $\psi = (\psi_1 \;\; \psi_2)^T \in L^2\left([0, T], \mathbb{C}^2\right)$ solves the Riccati-Volterra equation*

$$\psi = uK_Z + \left(\psi B + \frac{1}{2} A(\psi) \right) \star K_Z \, . \tag{5.14}$$

Using the form of K_Z and of the coefficients $b(z)$ and $a(z)$ given by (5.12) *and* (5.13)*, we obtain*

$$\psi_1 = u_1\,, \tag{5.15}$$

$$\psi_2 = u_2 K + K \star \mathcal{R}_\Psi(\psi)\,, \tag{5.16}$$

where we define

$$\mathcal{R}_\Psi(\psi) = \frac{1}{2}m^2(\psi_1^2 - \psi_1) + (b + m\psi_1\rho a)\psi_2 + \frac{a^2}{2}\psi_2^2 \qquad \textbf{and} \qquad \mathcal{R}_\Phi(\psi_2) = \beta\psi_2\,.$$

Then, the Laplace transform of Z_T is given by

$$\mathbb{E}[e^{uZ_T}] = e^{\phi(T)+\chi(T)V_0+u_1Y_0}\,, \tag{5.17}$$

where

$$\phi' = \frac{d}{dt}\phi = \mathcal{R}_\Phi(\psi_2)\,, \qquad \chi' = \frac{d}{dt}\chi = \mathcal{R}_\Psi(\psi)\,,$$

and

$$\phi(0) = 0\,, \qquad \chi(0) = u_2\,.$$

Proof. Cfr Appendix 10.4. □

However, we are especially interested in the characteristic function of the log-cushion X_t which can be obtained from the dynamic of Y_t using equation (3.5). Therefore, we now study the following affine Volterra process $\widetilde{Z} = (X, v)$ and obtain the next Corollary 5.1 with the same assumptions as in the previous theorem.

Corollary 5.1. *The Laplace transform of the the log-cushion X_T at horizon T associated with the affine Volterra process $\tilde{Z}$ is given by*

$$\mathbb{E}[e^{u_1X_T}] = e^{\phi(T)+\chi(T)V_0+u_1(X_0+(r+m(\mu-r))t)}\,, \tag{5.18}$$

with ϕ and χ defined by

$$\phi' = \frac{d}{dt}\phi = \mathcal{R}_\Phi(\psi_2)\,, \qquad \chi' = \frac{d}{dt}\chi = \mathcal{R}_\Psi(\psi)\,,$$

where $\mathcal{R}_\Phi(\psi_2)$ and $\mathcal{R}_\Psi(\phi)$ are defined in Theorem 5.1 and with initial conditions defined by

$$\phi(0) = 0\,, \qquad \chi(0) = 0\,.$$

The process $\psi = (\psi_1 \;\; \psi_2)^T \in L^2\left([0,T], \mathbb{C}^2\right)$ is now the solution of the following Riccati-Volterra equation

$$\psi_1 = u_1\,, \tag{5.19}$$

$$\psi_2 = K \star \mathcal{R}_\Psi(\psi) = K \star \left(\frac{1}{2}m^2(u_1^2 - u_1) + (b + mu_1\rho a)\psi_2 + \frac{a^2}{2}\psi_2^2\right). \tag{5.20}$$

Proof. Cfr Appendix 10.5. □

It is important to note that we only consider here the unconditional characteristic function of affine Volterra processes at time $s = 0$. Indeed, Theorem 5.1 and Corollary 5.1 do not hold anymore at a later time s since we cannot write the conditional characteristic function $\mathbb{E}[e^{u_1 X_T}|\mathcal{F}_s]$ as a linear function of $\phi(\cdot)$ and $\chi(\cdot)$. Based on this Corollary 5.1, we can easily recover the characteristic function of the log-cushion under the Heston model, which is given by equations (5.3) and (5.4) and under the rough Heston model, given by (3.12) and (3.9). It suffices to take $u_1 = iz, a = \nu$, $\beta = \lambda\theta$ and $b = -\lambda$ with $K \equiv 1$ as convolution kernel in the Heston model and $K(t) = t^{\alpha-1}/\Gamma(\alpha)$ in the rough Heston model. Moreover, from Ackermann *et al.* (2020), we note that we could extend the results above by considering a time-dependent mean-reversion level $\theta(t)$ instead of the constant θ and hence work with the generalized rough Heston model of El Euch & Rosenbaum (2019).

We finally conclude that the class of Volterra processes tends to be suitable for building CPPI strategies that are analytically tractable through their characteristic function. Such affine Volterra processes allow to easily derive CPPI properties under various market conditions. Indeed, recent empirical studies suggest that the memory properties of market fears are unstable and change over time, leading to fluctuating behavior of financial markets as argued by Caporale *et al.* (2018). Following Cadoni *et al.* (2017), roughness is also associated with risks in pension fund portfolios where such CPPI strategies are often used. Affine Volterra processes are also useful for studying CPPI strategies based on underlying assets related to the commodity market, cfr Benth *et al.* (2020).

5.3. *Black and Scholes model*

Finally, for the sake of comparison with what has already be done in the literature, we analyze the characteristic function of the log-cushion in the B&S model. In this B&S model, we have that the log-cushion dynamic can be rewritten, in a similar way as in equation (3.5), by

$$dX_t = (r + m(\mu - r))dt - \frac{1}{2}m^2\sigma^2\,dt + m\sigma dW_t\,. \tag{5.21}$$

Hence, it directly comes that the characteristic function of the log-cushion is given by

$$\Phi_0^X(T,z) = \mathbb{E}\left[e^{izX_T}\middle|\,X_0\right] = \exp\left\{iz\Big(X_0 + T\left(r + m(\mu - r)\right)\Big) - \frac{1}{2}m^2(z^2 + iz)\sigma^2\,T\right\}. \tag{5.22}$$

There are no latent variables in this model which implies that we do not need to use a particle filter and that we can directly apply the Metropolis-Hasting algorithm with unknown parameters $\Theta = (\mu, \sigma)$. Since the log-return follows

$R_j \sim N\left((\mu - \sigma^2/2)\Delta, \sigma^2\Delta\right)$, the log-likelihood is now directly obtained by

$$\ln f(r \mid \vartheta) = -\frac{n}{2}\ln(2\pi\sigma^2\Delta) - \ln\left(\frac{\sum_{j=1}^{n}\left(r_j - (\mu - \frac{\sigma^2}{2})\Delta\right)^2}{2\sigma^2\Delta}\right).$$

Again with $K = 20\,000$ iterations, we find a log-likelihood of 3380.25 and the following parameter estimates :

Table 3. Parameter estimates of the B&S model and std. err. of these estimates.

	$\widehat{\mu}$	$\widehat{\sigma}$
Estimators PMCMC	0.1099	0.1988
PMCMC std. err.	0.0657	0.0042

The log-likelihood is the lowest of the analyzed models, leading to the poorest statistical fit. We obtain a very precise estimator of the volatility σ, which is lower compared to the mean levels derived in the two previous models. The mean rate of return μ is also lower in the B&S model and has a quite high standard error.

5.4. *(Fractional) Riccati equations*

In order to obtain the characteristic function of the log-cushion in the rough Heston model, we need to solve the fractional Riccati equation (3.9). Based on Momani & Shawagfeh (2006), we use an Adomian decomposition method combined with Padé approximants to obtain numerically the solution of such fractional Riccati equations. This method is highly effective and stable in order to capture the essential behavior of the solution $\psi(t,u)$ in the fractional Riccati case and provides solutions that are consistent with the numerical scheme described in the classical paper of Diethelm *et al.* (2002) for finding solutions of fractional differential equations. For the Heston model, we need to solve the ordinary Riccati equation (5.4). No analytical solution can be found to this first-order nonlinear ODE and we hence also resort to the Adomnian method of Momani & Shawagfeh (2006) with $\alpha = 1$ to derive numerically the solution $\psi(t,u)$.

We now show how to compute the moments of different orders for the portfolio value P_T at maturity. We mainly consider the Heston and rough Heston models, which are two important members of our class of affine Volterra processes $\widetilde{Z}$. We also compare these results under the B&S framework for the log-cushion dynamic.

6. Moments

From the characteristic function of the log-cushion, the moments of order k of the cushion C_t can be directly obtained by imposing $iz = k$. Indeed, we have

$$\Phi_X(T, -ki) = \mathbb{E}\left[e^{kX_T}\right] = \mathbb{E}\left[e^{k\log C_T}\right] = \mathbb{E}\left[C_T^k\right]. \tag{6.1}$$

We consider here the situation at time $s = 0$ where the initial amount in the fund P_0 is 100 and where the guaranteed amount $G(= F_T)$ at maturity $T = 1$ is 95. We find that $F_0 = 95e^{-1r} = 94.77$ and hence that $C_0 = P_0 - F_0 = 5.23$.

For the multiple, applying the extreme value approach of Bertrand & Prigent (2016), we are able to provide an upper bound of the multiple m based on our dataset of past log-returns for the S&P500. Considering a management period of 1 month (21 days) and a risk tolerance ε of 0.5%, we find empirically an upper bound $m \leq 4.1117$ such that the shortfall probability satisfies $P\left[\exists\, j \in [1, n] : C_{t_j} \leq 0\right] \leq \epsilon$ by following the methodology of these authors. We therefore choose a value $m = 4$ satisfying this upper bound such that the worst daily return anticipated by the fund manager over the investment horizon is 25%. Using the models introduced above, we are able to find the k^{th} order moment of the cushion value C_T and we hence obtain the following Table 4 describing the expectation, standard deviation/volatility, skewness and kurtosis of the portfolio value P_T at maturity, using the relation $\mathbb{E}[P_T^k] = \mathbb{E}[(C_T + F_T)^k]$:

Table 4. Comparison of the first four moments of P_T based on the characteristic function of the log-cushion under each of the three estimated models.

	Expectation	Volatility	Relative Skewness	Relative Kurtosis
B&S	103.0599	7.5695	3.6458	33.5037
Heston	104.0626	8.1671	2.7833	55.3041
Rough Heston	104.2598	6.2334	2.1259	68.7292

First, we have logically that the expected value of the fund is lower in the B&S model due to the lower rate of return μ. We also see that volatility and skewness are lower in the rough Heston model due to the much lower speed of mean reversion λ. However, the main difference comes from the 4^{th} moment which is higher in the rough Heston case and lower in the B&S model. These differences can be explained by the absence of leverage effect in the B&S model and by the roughness property of the variance process under the rough Heston case, as we will see below with Table 5. Note that moments of the fund obtained via simulations such as in Prigent & Bertrand (2003) are consistent with the values derived from our method based on the characteristic function of the log-cushion. Moreover, the methodology derived in this paper overcomes the instability and slowness of these simulations and allows to accurately and efficiently generate the moments of the fund value P_T.

Finally, we want to emphasize the impact of rough volatility on the portfolio's moments. We therefore impose for the rough Heston model the same parameters $\mu, \lambda, \theta, \nu, \rho$ as in the Heston model (cfr Table 2) and we consider for the roughness index α a value of 0.75. For the B&S model, we also take $\mu = 0.1392$ as in the Heston model and σ equal to the average Heston volatility $\frac{1}{t}\int_{s=0}^{t} \mathbb{E}[\sigma_s]ds = 0.2156$. Using these comparable parameters, we obtain the following Table 5. First, we have

Table 5. Comparison of the first four moments of P_T based on the characteristic function of the log-cushion under each of the three models with comparable parameters.

	Expectation	Volatility	Relative Skewness	Relative Kurtosis
B&S	104.0626	9.5189	4.3010	48.4466
Heston	104.0626	8.1671	2.7833	55.3041
Rough Heston	104.0626	8.1870	2.7220	116.7027

that the B&S model provides a volatility and a skewness that are higher than in the other models. This is due to the negative correlation ρ of the Heston and rough Heston models which decreases their moment values. Therefore, since the B&S model does not take into account the leverage effect, it tends to overestimate the moments of the fund P_T. Concerning the kurtosis, the absence of heavy tail in the B&S model compensates for the absence of leverage effect and we hence obtain a lower 4^{th} moment compared with the two other models. Next, the main difference between the Heston and rough Heston models comes from the 4^{th} moment, with a much higher kurtosis in the rough Heston case. The roughness of the volatility hence strongly impacts the tail of the portfolio distribution and the occurrence probability of extreme events affecting the CPPI value. Indeed, as explained in Paulot & Lacroze (2009), CPPI is very sensitive to tails events and its value distribution depends mainly on the mean volatility and on the left tail of the underlying distribution. Hence, this rough behavior of volatility is crucial and must be taken into account in order to better assess the tail of the distribution and the true CPPI properties.

In a similar way as for the calculation of the moments of the portfolio value P_T, we now show that we can derive efficiently and consistently several risk measures as well as the density of P_T based on the characteristic function of the log-cushion. Results will be obtained both with the true estimated parameters of each model as well as with the comparable parameters based on the Heston model as in Table 5.

7. Risk Measure and probability density

Based on Artzner *et al.* (1999), we define the Value-at-Risk (VaR) as the ε-quantile of the portfolio value at the term of a chosen time horizon T. This risk measure is used to appraise the shortfall risk and despite that it is not a coherent risk measure (cfr Artzner *et al.* (1999)), the Value-at-Risk still remains an essential tool for asset allocation. If $\varepsilon \in [0,1]$ is the maximum shortfall probability accepted by the investor, then the VaR is defined as the shortfall level, q, such that

$$P(P_T \leq q) = \varepsilon \quad \Longleftrightarrow \quad P(C_T \leq q - F_T) = \varepsilon \quad \Longleftrightarrow \quad P(X_T \leq \log(q - F_T)) = \varepsilon \tag{7.1}$$

where $X_T = \log C_T$. If we then denote the probability density function of X_T by $f_T(\cdot)$, this relation becomes

$$\int_{-\infty}^{\log\left(q-F_0e^{rT}\right)} f_T(x)\,dx = \varepsilon\,. \tag{7.2}$$

Another common measure of risk is the Tail Value-at-Risk (TVaR), denoted tv, which is the expected shortfall level if the portfolio value breaches the VaR q,

$$\begin{aligned} tv = \mathbb{E}[P_T|P_T \le q] \quad &\Longleftrightarrow \quad tv = \mathbb{E}\left[C_T + F_0e^{rT} \,\middle|\, C_T \le q - F_0e^{rT}\right] \\ &\Longleftrightarrow \quad tv = \mathbb{E}\left[e^{X_T} \,\middle|\, X_T \le \log(q - F_0e^{rT})\right] + F_0e^{rT} \end{aligned} \tag{7.3}$$

Equation (7.3) can be rewritten in terms of the pdf $f_T(\cdot)$ as follows

$$tv = \frac{1}{\varepsilon}\int_{-\infty}^{\log\left(q-F_0e^{rT}\right)} e^x\, f_T(x)\,dx + F_0e^{rT}\,. \tag{7.4}$$

The TVaR is a coherent risk measure, also called expected shortfall and can identically be defined as the conditional tail expectation when applied to continuous random variables.

The probability distribution of the log-cushion X_T (conditionally to X_0 and V_0) under the above models is not analytically determined (except for the B&S model). However, its characteristic function $\Phi_X(T, z)$, which is also the Fourier Transform of its density, has a quasi-closed form under these models. By inverting numerically the characteristic function of X_T, it is hence possible to determine its density of probability and to compute numerically the VaR and TVaR by equations (7.2) and (7.4). This numerical scheme, adapted from Hainaut (2011), relies on the Fast Fourier Transform (FFT) algorithm and is detailed in Appendix 10.6.

7.1. *Application*

7.1.1. *Comparable parameters*

The log-cushion density obtained numerically from the FFT algorithm (cfr Appendix 10.6) is first plotted below in Fig. 1 for each of the studied models based on the Heston parameters (as used in Table 5). The number of steps involved in the FFT algorithm is set to $N = 2048$. We first observe that the log-cushion is normally distributed under the B&S model, which explains the shape of the blue curve in Fig. 1. Compared with the other models, we see that the probability density function of the B&S log-cushion is shifted to the right with more weight attributed to high values of the log-cushion. We also see that log-cushion values are more dispersed around the mean in the B&S model. This explains the higher volatility $\sigma[P_T]$ of the portfolio value in Table 5.

The density functions of the log-cushion under the Heston and rough Heston models are extremely similar. Both are negatively-skewed with fat left tails. First, this

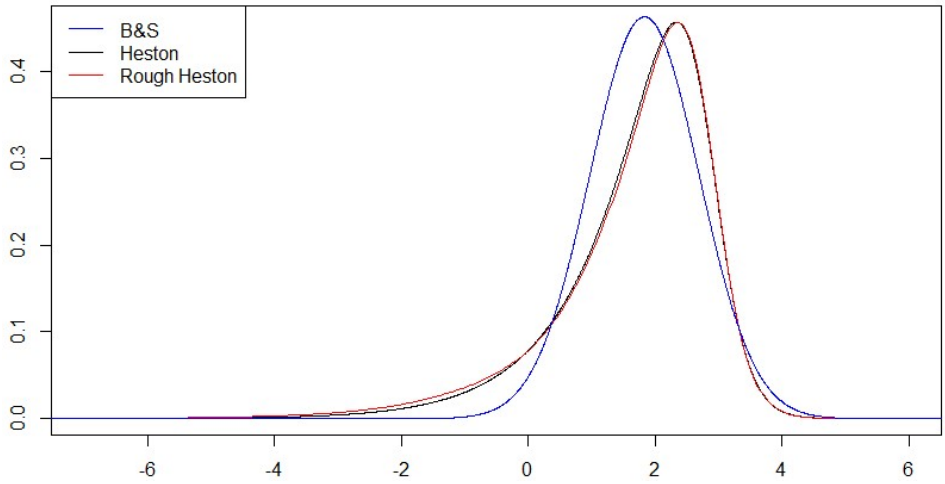

Fig. 1. Density of the log-cushion for the three models with comparable parameters and $m = 4$.

negative skewness of the log-cushion explains why the skewness of the portfolio value P_T in Table 5 is lower than in the B&S model when taking the exponential of the distribution (but still positive since the effect of the exponential function on the skewness overcomes the negative skewness of the log-cushion). Secondly, the fatter left tail observed for the black and red curves below is the reason why we obtain a higher kurtosis in Table 5, compared with the B&S model. Finally, based again on Table 5, we also observe that this is logical to obtain very similar densities between the Heston and rough Heston models since the three first moments are extremely close to each other. Only the kurtosis differs between these two models, which is indeed confirmed on Fig. 1 with a fatter left tail for the rough Heston in red compared with the Heston curve in black. A higher multiplier value m would have emphasized these effects.

Based on the probability density function of the log-cushion, we can now derive its quantiles and hence use formula (10.12) to compute the VaR q of the portfolio value P_T. We then obtain the following Table 6 describing five percentiles of interest for P_T (mainly describing the left tail of the distribution) with $m = 4$:

Table 6. Comparison of different quantiles of the portfolio value P_T between models (comparable parameters).

	0.5%	**1%**	**5%**	**25%**	**50%**
B&S	95.6766	95.8388	96.5130	98.4903	101.2466
Heston	95.0566	95.1140	95.5953	98.2514	102.1060
Rough Heston	95.0272	95.0674	95.4746	98.0959	101.9930

This Table 6 confirms and details Fig. 1 of the log-cushion density. The rough Heston

model tends to have the lowest values for small percentiles (and hence be the most risky) since it has the fattest left tail, closely followed by the Heston model. We also clearly see that the B&S model exhibits the highest values for small quantiles, which is again explained by its lower kurtosis. The trend reverses for higher quantiles such as the median where we obtain larger values for the Heston and rough Heston models compared with the B&S model. We now turn to the TVaR of the portfolio value which is defined by formula (7.4) and we obtain the following Table 7 for all our models with $m = 4$:

Table 7. Comparison of the TVaR at levels 0.5%, 1%, 5% and 25% of P_T between models (comparable parameters).

	0.5%	**1%**	**5%**	**25%**
B&S	95.5316	95.6478	96.1108	97.2603
Heston	95.0284	95.0569	95.2950	96.5821
Rough Heston	95.0120	95.0310	95.2182	96.4484

By definition, we have that the TVaR is below the VaR at corresponding levels. Again, we confirm that the rough Heston model has the fattest left tail and is the most risky with significant probability attributed to very small values of P_T, while the B&S portfolio value exhibits the highest TVaR for small percentile levels. Finally, it can again be confirmed that the values of VaR and TVaR derived in Table 6 and Table 7 are consistent and close to the values obtained from simulations. However, simulation-based methods (Monte-Carlo, Hybrid scheme, ...) are way more slow and less stable than working directly with the characteristic function of the log-cushion, especially for the rough Heston model due to the non-Markovian nature of its variance process.

7.1.2. *True estimated parameters*

We now derive the log-cushion density (Fig. 2) as well as the VaR and TVaR of the portfolio value P_T (Tables 8 and 9) based on the original parameters of each model as in Table 4 since these parameters are those of true interest.

Table 8. Comparison of different quantiles of the portfolio value P_T between models with the true estimated parameters.

	0.5%	**1%**	**5%**	**25%**	**50%**
B&S	95.7578	95.9212	96.5856	98.4303	100.8681
Heston	95.0566	95.1140	95.5953	98.2514	102.1060
Rough Heston	95.1368	95.2596	96.1420	99.7313	103.4551

Despite having the highest kurtosis in Table 4, the rough Heston model with the true estimated parameters is less risky than the Heston model with higher risk measures in the rough Heston (VaR, TVaR) for small quantiles. Indeed, this can be explained by the fact that the rough Heston model has a substantially lower

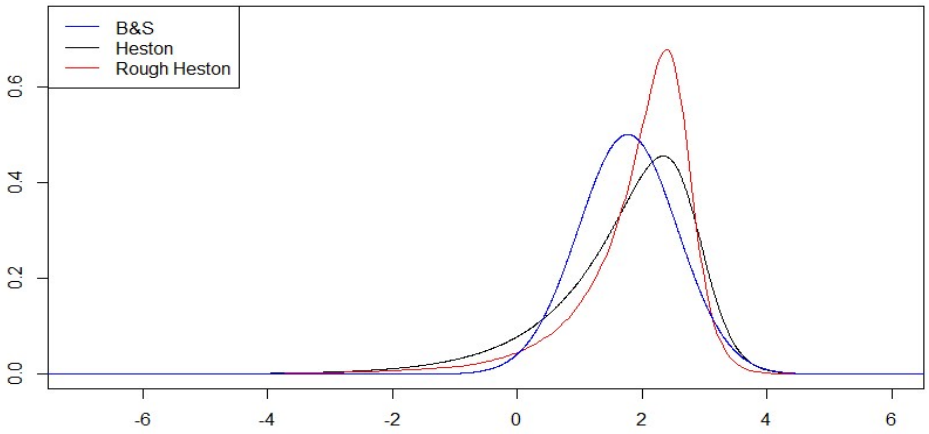

Fig. 2. Density of the log-cushion for each model with the true estimated parameters and $m = 4$.

Table 9. TVaR at levels 0.5%, 1%, 5% and 25% of P_T for each model with the true estimated parameters.

	0.5%	**1%**	**5%**	**25%**
B&S	95.6096	95.7222	96.1842	97.2726
Heston	95.0284	95.0569	95.2950	96.5821
Rough Heston	95.0699	95.1320	95.5921	97.6052

volatility and skewness in Table 4 compared with the Heston model, which also impacts the riskiness and gap risk of the CPPI strategy (as we will see in the next section). The impact of the kurtosis on these two models can however be seen in Tables 8 and 9 with lower differences between risk measures at small levels (0.5%, 1%, 5%) and higher differences at larger levels (25%, 50%). Fig. 2 confirms these findings.

8. Discrete-time CPPI

Since we have assumed continuous trading on the whole investment horizon $[0, T]$, we cannot take into account the gap risk, *i.e.* the risk of violating the floor protection. We can indeed observe in Table 6 that the final value of the portfolio P_T is systematically above the guarantee $G = 95$, even for very small quantiles. This gap risk is caused by liquidity constraints and steep drops in the risky asset occurring before the fund manager can rebalance the portfolio. It therefore needs to be managed. Such gap risk is discussed thoroughly in Cont & Tankov (2009) and in Bertrand & Prigent (2016). Nevertheless, both liquidity constraints and gap risk can be modeled in the setup of Balder *et al.* (2009) where the price dynamic of the risky asset is again described by a continuous-time stochastic process but where trading is now restricted to discrete time. In their framework,

they consider the sequence τ^n of equidistant refinements of the interval $[0,T]$, *i.e.* $\tau^n = \left\{t_0^n = 0 < t_1^n < \ldots < t_{n-1}^n < t_n^n = T\right\}$. This sequence represents the effective trading times and as above, we consider a management period of one month so that $n = 12$ (since T=1). Following Balder *et al.* (2009), the self-financing condition of the CPPI portfolio implies the following recursive relation for the cushion with $k = 1, \ldots, n-1$:

$$C_{t_{k+1}^n} = \begin{cases} C_{t_k^n}\left(m\frac{S_{t_{k+1}^n}}{S_{t_k^n}} - (m-1)e^{rT/n}\right) & \text{if } C_{t_k^n} > 0 \\ C_{t_k^n}\, e^{rT/n} & \text{if } C_{t_k^n} \leq 0. \end{cases} \tag{8.1}$$

Balder *et al.* (2009) consider that the price dynamic S_t simply follows a geometric Brownian motion and hence, they manage to derive closed-form formula for the shortfall probability $P^{SF} = P(\exists k \in [1,n] : C_{t_k^n} \leq 0)$, for the expected shortfall $ESF = \mathbb{E}\left[-C_{t_n^n} \,\middle|\, \exists k \in [1,n] : C_{t_k^n} \leq 0\right]$ and for the gap risk $GPR = \mathbb{E}\left[-C_{t_n^n}\, \mathbb{1}_{\left\{\exists k \in [1,n]\,:\, C_{t_k} \leq 0\right\}}\right]$. In order to handle and compute such gap risk measures associated with our Heston and rough Heston models, we need to simulate the price process in (8.1) under each of these two models since no closed-form formula exist in such cases. For the Heston model, well known simulation techniques exist (cfr Lord *et al.* (2010)). For the rough Heston, we again consider the time-efficient simulation scheme of Abi Jaber (2019) based on a lifted version of the Heston model, which appears to be extremely fast and accurate. We first obtain the following Table 10 with the comparable parameter estimates used in Table 5 :

Table 10. Shortfall probability, Expected shortfall and Gap risk for the three models with comparable parameters.

	P^{SF}	ESF	Gap risk
B&S	1.08×10^{-5}	0.24237	2.62×10^{-6}
Heston	0.0228	0.5100	0.0116
Rough Heston	0.0438	0.8125	0.0356

We clearly see that the rough Heston model provides the highest risk measures due to its fatter left tail. The B&S CPPI strongly underestimates the gap risk and gives measures way below the two other models. Moreover, we have the following Table 11 giving these different risk measures based on the true estimated parameters :

Table 11. Shortfall probability, Expected shortfall and Gap risk for the three models with $m = 4$ and the true estimated parameters.

	P^{SF}	ESF	Gap risk
B&S	1.65×10^{-6}	0.1990	3.28×10^{-7}
Heston	0.0228	0.5100	0.0116
Rough Heston	0.0053	0.4373	0.0025

What is fundamental to note is that the rough Heston model with the true estimated parameters provides a shortfall probability in accordance with the empirical

one associated with a $m = 4$. Indeed, recall from Section 6 that the estimated shortfall probability ε based on the empirical log-return data with $m = 4$ is equal to 0.5%. Hence, we see that the B&S model strongly underestimates the shortfall probability of the CPPI strategy while the Heston model overestimates it and tends to be too risky. The fact that the rough Heston model manages to remarkably reproduce such empirical shortfall probability means that rough volatility models indeed better reproduce tail events and are more consistent with the gap risk derived from empirical data of log-returns. This again confirms the importance of taking into account the roughness of volatility when considering and assessing CPPI strategies. Note that the client of a CPPI fund may be insured against this gap risk in such a way that he can recover from the bank the loss made if the fund breaks the floor. In this case, the share of a CPPI fund is a financial product with an optional component, *i.e.* the sum of a self-financing portfolio corresponding to the uninsured CPPI strategy and a put option with discounted payoff $-C_T \mathbb{1}_{\left\{\exists k \in [1,n] \,:\, C_{t_k} \leq 0\right\}}$. Practically, our methodology allows to better assess the gap risk since it provides a better modeling of the tails of the CPPI distribution and since it is more consistent with financial data. Clients and practitioners can hence better hedge against this gap risk. Moreover, transaction costs could also be taken into consideration with this discrete setting, cfr Balder *et al.* (2009).

9. Conclusion

This paper proposes to derive and study the properties of CPPI strategies based on the characteristic function of the log-cushion. The class of affine Volterra processes appears to be particularly adapted for building such CPPI strategies in frictionless markets since their log-cushion's characteristic function is given in quasi-closed form and can be evaluated rapidly using numerical schemes. This method allows to generalize results previously established in the literature for a large class of models, especially when the variance process associated with the risky asset is non-Markovian in the current variance state. Through the choice of the coefficients a and b as well as the convolution kernel K of affine Volterra processes, various and more realistic dynamics can be envisaged for the underlying risky asset on which the CPPI strategy is defined. In particular, we investigate the CPPI strategy under rough volatility with the rough Heston model (using a power law kernel K) since this model is known for being extremely consistent with past volatility time series. We then show how to obtain effectively and accurately very consistent results from the characteristic function of the log-cushion, such as the moments, the density, several risk measures as well as some gap risk measures for the portfolio value P_T. Moreover, the Heston model which belongs as well to the class of affine Volterra processes (with an identity kernel), is also studied in this paper and we again get results in a more effective and accurate way using the characteristic function of the log-cushion compared with classical simulation-based methods. For the sake of comparison, this characteristic function is also given under the simple B&S framework.

These three models are estimated directly under the real probability measure based on the PMCMC procedure of Andrieu *et al.* (2010) from a dataset of S&P500 daily log-returns. In particular, this PMCMC algorithm is adapted for the rough Heston model so as to take into account the non-Markovianity of its variance process. This allows to deviate from the existing calibration procedure of the rough Heston in the literature, exclusively based on risk-neutral data, and to provide a better statistical fit of the past time series of log-returns. From this econometric estimation of the considered models, we emphasize the importance of taking into account the roughness of volatility for providing a better modeling of the tail of the CPPI distribution. This roughness property of volatility has indeed a strong impact on the kurtosis of the CPPI distribution and since CPPI strategy is very sensitive to tail events, we show that the rough Heston model enables to study more accurately the true properties of the portfolio value at maturity. These effects are confirmed with the analysis of the log-cushion density under each model as well as with the study of several risk measures such as the VaR and TVaR. Finally, in a more practical way, the rough Heston better models the gap risk associated with the CPPI strategy compared with the Heston and B&S models. It therefore provides a better protection of the guaranteed amount at maturity for the client and allows the issuer to build a more accurate hedging strategy.

10. Appendix

10.1. *Fractional Calculus*

We define the fractional integral of order $r \in (0,1)$ of a function f as

$$I^r f(t) = \frac{1}{\Gamma(r)} \int_0^t (t-s)^{r-1} f(s)\, ds\,,$$

whenever the integral exists, and its fractional derivative of order $r \in (0,1)$ as

$$D^r f(t) = \frac{1}{\Gamma(1-r)} \frac{d}{dt} \int_0^t (t-s)^{-r} f(s)\, ds\,,$$

whenever it exists. If we take the power-law kernel $K(t) = t^{r-1}/\Gamma(r)$, the fractional integral and derivative are given by the following convolution operator

$$I^r f(t) = (K \star f)(t)\,, \qquad D^r f(t) = \frac{d}{dt}\left(I^{1-r} f(t)\right).$$

10.2. *Proof of Theorem 3.1.*

The proof closely follows the one of Gatheral & Keller-Ressel (2019) and expands their results in the context of CPPI. Let

$$G_s = (g \star \xi)_s(T,u) = \int_s^T g(T-r,u)\xi_s(r)dr\,, \tag{10.1}$$

$$M_s = \exp\left(uY_s + G_s\right). \tag{10.2}$$

Hence, it directly comes from (3.6) that M is a martingale. It is also shown in Gatheral & Keller-Ressel (2019) that G can be rewritten as an Itô process of the form

$$G_s = \int_0^T g(T-r,u)\xi_0(r)dr - \int_0^s g(T-r,u)V_r\,dr + \int_0^s h_r(T,u)dW_r\,, \qquad (10.3)$$

where

$$h_s(T,u) = (g\star\eta)_s(T,u) = \int_s^T g(T-r,u)\eta_s(r)dr\,.$$

This equation 10.3 for G is obtained using the stochastic Fubini theorem which requires the *Assumption 2.1* of Gatheral & Keller-Ressel (2019) imposing the two following conditions on $\eta_s(\cdot)$:

(a) For $dt\otimes d\mathbb{P}$-almost all (t,ω), it hold that $t\mapsto\eta_s(s+t,\omega)$ is non-negative and decreasing on $(0,T)$
(b) For any $T>0$, the following integrability condition holds almost surely :

$$\int_0^T\left(\int_0^T \eta_s(r)^2 ds\right)^{1/2} dr < \infty\,.$$

We now expand their results and show that the CGF is still affine when considering the following dynamic for Y (cfr equation (3.5)) :

$$dY_s = -\frac{1}{2}m^2\,V_s\,ds + m\sqrt{V_s}\,dW_s\,.$$

Then, applying Itô's lemma to $M_s = \exp(uY_s + G_s)$, we have that

$$\begin{aligned}\frac{dM_s}{M_s} &= (dW_s \text{ terms})\\ &\quad + \left(\frac{1}{2}m^2(u^2-u)V_s - g(T-s,u)V_s + mu\rho\sqrt{V_s}\,h_s(T,u) + \frac{1}{2}h_s(T,u)^2\right)ds\,.\end{aligned}$$

Since we know from Section 2 that $\eta_s(T) = \sqrt{V_s}\,\kappa(T-s)$, we find the following simplification for $h_s(T,u)$, similar as the one derived in Gatheral & Keller-Ressel (2019) :

$$h_s(T,u) = (g\star\eta)_s(T,u) = \sqrt{V_s}\int_0^{T-s} g(T-s-r,u)\kappa(r)dr = \sqrt{V_s}\,(g\star\kappa)(T-s)\,.$$

Therefore, if we define

$$R_v(m,u,w) = \frac{1}{2}m^2(u^2-u) + m\rho uw + \frac{1}{2}w^2\,, \qquad (10.4)$$

we find that

$$\frac{dM_s}{M_s} = (dW_s \text{ terms}) + \left(R_v\left(m,u,(g\star\kappa)(T-s)\right) - g(T-s,u)\right)V_s\,ds\,.$$

In order to have that M is a local martingale, we need to cancel the terms in ds and we hence find the following expression for $g(\cdot, u)$,

$$g(t,u) = R_v\left(m, u, (g \star \kappa)(t,u)\right) = R_v\left(m, u, \int_0^t \kappa(t-r)g(r,u)dr\right), \tag{10.5}$$

Finally, following Gatheral & Keller-Ressel (2019), one can show that M is a true martingale and then, expression 10.5 enables to compute the CGF of the forward variance model (Y, ξ) using

$$\log \mathbb{E}\left[e^{u(Y_T - Y_s)}|\mathcal{F}_s\right] = \int_s^T g(T-r,u)\xi_s(r)dr\,. \tag{10.6}$$

□

10.3. *Algorithms*

Algorithm 1 Particle filtering of the rough Heston model.

Initial step : draw N values of $v_0^{(i)}$ for $i = 1, \cdots, N$ from the initial distribution $f(v_0)$, which is assumed to be uniform $\mathcal{U}_{[0,0.36]}$.

Main procedure :

for $j = 1$ to n **do**

Prediction step :

Draw a sample $\Delta w_j^{2(i)}$ from a $N(0, \sqrt{\Delta})$, $i = 1, \cdots N$.

Update $v_j^{(i)}$ using the relation :

$$v_j^{(i)} = v_0^{(i)} + \sum_{k=0}^{j-1} \frac{(t_j - t_k)^{\alpha-1}}{\Gamma(\alpha)} \lambda\left(\theta - v_k^{(i)}\right)\Delta + \sum_{k=0}^{j-1} \frac{(t_j - t_k)^{\alpha-1}}{\Gamma(\alpha)} \nu \sqrt{v_k^{(i)}}\, \Delta w_{k+1}^{2(i)}$$

Correction step :

The particle $u_j^{(i)} = \left(v_k^{(i)}, \Delta w_k^{2(i)}\right)_{k=1:j}$ has a probability of occurrence

$$p_j^{(i)} = \frac{f(r_j \,|\, u_j^{(i)})}{\sum_{i=1:N} f(r_j \,|\, u_j^{(i)})}$$

where

$$f(r_j \,|\, u_j^{(i)}) = \phi\left(\frac{r_j - \left(\mu - \frac{v_{j-1}^{(i)}}{2}\right)\Delta - \rho\sqrt{v_{j-1}^{(i)}}\,\Delta w_j^{2(i)}}{\sqrt{1-\rho^2}\sqrt{v_{j-1}^{(i)}}\sqrt{\Delta}}\right)$$

Resampling step :

Resample with replacement N particles with importance weights $p_j^{(i)}$.

The initial importance weights are set to $p_j^{(i)} = 1/N$.

end for

Algorithm 2 Metropolis Hastings algorithm.

Main procedure :

for $j = 1$ to n **do**

Simulate $\vartheta^{'} \sim q(\vartheta^{'} \,|\, \vartheta_t)$

Take

$$\Theta_{t+1} = \begin{cases} \vartheta^{'} & \text{with probability } \rho(\vartheta_t, \vartheta^{'}) \\ \vartheta_t & \text{with probability } 1 - \rho(\vartheta_t, \vartheta^{'}) \end{cases}$$

where $\rho(\vartheta_t, \vartheta^{'})$ is the acceptance probability

$$\rho(\vartheta_t, \vartheta^{'}) = \min\left\{ \frac{f(\vartheta^{'} \,|\, r)}{f(\vartheta_k \,|\, r)} \frac{q(\vartheta_k \,|\, \vartheta^{'})}{q(\vartheta^{'} \,|\, \vartheta_k)}, 1 \right\}$$

end for

10.4. *Proof of Theorem 5.1.*

This proof follows Keller-Ressel *et al.* (2018) and expands their results in the context of CPPI. For an investment horizon T, we also define $M_t = e^{U_t}$, with U_t given by

$$\begin{aligned} U_t &= \phi(T-t) + \chi(T)V_0 - \int_0^t \chi'(T-s)V_s ds + \int_0^t \psi_2(T-s)dL_s + \psi_1(T-s)Y_t \\ &= \phi(T-t) + \chi(T)V_0 - \int_0^t \chi'(T-s)V_s ds + \int_0^t \psi_2(T-s)dL_s + u_1 Y_t\,, \quad (10.7) \end{aligned}$$

since $\psi_1 = u_1$ due to the form (5.15) and where $dL_t = (\beta + bV_s)\,ds + \left(0 + a\sqrt{V_s}\right) d\widehat{W}_s$ as in Section 5.2 to ensure that the process $Z = (Y, V)$ is an affine Volterra process. Using Itô's lemma on $M_t = e^{U_t}$, we have

$$\begin{aligned} \frac{dM_t}{M_t} =& -\phi'(T-t) - \chi'(T-t)V_t\,dt + \psi_2(T-t)(\beta + bV_t)dt + \frac{1}{2}\psi_2(T-t)^2 a^2 V_t\,dt \\ &+ \frac{1}{2}m^2(u_1^2 - u_1)V_t\,dt + \rho\psi_2(T-t)\left(0 + a\sqrt{V_t}\right)u_1 m\sqrt{V_t}\,dt + (dW_t \text{ terms})\,, \end{aligned}$$

which gives

$$\frac{dM_t}{M_t} = \left(-\phi'(T-t) + \mathcal{R}_\Phi(\psi_2(T-t))\right)dt + \left(-\chi'(T-t) + \mathcal{R}_\Psi(\psi(T-t))\right)V_t\,dt + (dW_t \text{ terms})\,,$$

where we define

$$\mathcal{R}_\Phi(\psi_2) = \beta\psi_2 + 0\,,$$

and

$$\begin{aligned} \mathcal{R}_\Psi(\psi) &= \frac{1}{2}m^2(\psi_1^2 - \psi_1) + (b + m\psi_1\rho a)\psi_2 + \frac{a^2}{2}\psi_2^2 \\ &= \frac{1}{2}m^2(u_1^2 - u_1) + (b + mu_1\rho a)\psi_2 + \frac{a^2}{2}\psi_2^2\,. \end{aligned}$$

Hence for M to be a local martingale on $[0,T]$, we find that $\phi' = \mathcal{R}_\Phi(\psi_2)$ and that $\chi' = \mathcal{R}_\Psi(\psi)$. Imposing that $\phi(0) = 0$ and $\chi(0) = u_2$ and using the definition of U_t as well as the form (5.16) of ψ_2, it is straightforward to show that

$$U_T = \phi(0) + \chi(0)V_T + u_1 Y_T = u_2 V_T + u_1 Y_T \,, \tag{10.8}$$

Since we assume that K satisfies (5.11) and that $u \in \mathbb{C}^2$ with Re $u_1 \in [0,1]$ and Re $u_2 \leq 0$, the Riccati-Volterra equation (5.16) has a unique global solution ψ_2 and M is a true martingale, as shown in Theorem 7.1. of Abi Jaber *et al.* (2019). Hence, since M is a true martingale, we have with $u = (u_1 \; u_2)$ and $Z = (Y \;\; V)^T$ that

$$\mathbb{E}[e^{uZ_T}] = \mathbb{E}[e^{u_2 V_T + u_1 Y_T}] = \mathbb{E}[M_T] = M_0 = e^{\phi(T) + \chi(T)V_0 + u_1 Y_0} \,.$$

□

10.5. *Proof of Corollary 5.1.*

We build the exact same proof as in Theorem 5.1. with the same assumption on K except that we now impose $u_2 = 0$ such that $\chi(0) = 0$. Hence, the terminal value U_T of the process U defined by (10.7) is now

$$U_T = \phi(0) + \chi(0)V_T + u_1 Y_T = u_1 Y_T \,.$$

Since M is still a true martingale when $u_2 = 0$, we have that

$$\mathbb{E}[e^{uZ_T}] = \mathbb{E}[e^{u_1 Y_T}] = \mathbb{E}[e^{U_T}] = \mathbb{E}[M_T] = M_0 = e^{\phi(T) + \chi(T)V_0 + u_1 Y_0} \,,$$

and the solution ψ now becomes

$$\begin{aligned} \psi_1 &= u_1 \,, \\ \psi_2 &= K \star \mathcal{R}_\Psi(\psi) \,. \end{aligned} \tag{10.9}$$

Finally, recall from (3.5) that the dynamic of the log-cushion is denoted X_t and is given by

$$dX_t = (r + m(\mu - r))\, dt + dY_t \,.$$

Hence, the Laplace transform of the affine Volterra process $\widetilde{Z} = (X, V)$ with $u_2 = 0$ becomes

$$\mathbb{E}[e^{u\widetilde{Z}_T}] = \mathbb{E}[e^{u_1 X_T}] = e^{\phi(T) + \chi(T)V_0 + u_1(X_0 + (r + m(\mu - r))t)} \,.$$

And finally the characteristic function of the log-cushion under the general affine Volterra process $\widetilde{Z}$ is obtained by replacing u_1 by iz.

□

10.6. *Fast Fourier Transform*

We present here the approach used to determine numerically the density of probability of the log-cushion X_T, which then allows to obtain the VaR and TVaR of the portfolio value V_T for each model. First, the characteristic function of X_T, denoted $\Phi_X(T,z)$, is by definition the Fourier Transform of the density $f_T(x)$ of X_T :

$$\Phi_X(T,z) = \mathbb{E}[e^{izX_T}] = \int_{-\infty}^{+\infty} e^{izx} f_T(x)\, dx\,.$$

Since we know the characteristic function of X_T for the B&S, Heston and rough Heston models, we can derive the density function $f_T(x)$ using the Fourier inversion theorem which states that

$$f_T(x) = \frac{1}{2\pi}\int_{-\infty}^{+\infty} \Phi_X(T,z)\, e^{-izx} dz = \frac{1}{\pi}\int_0^{+\infty} \Phi_X(T,z)\, e^{-izx}\, dz\,, \tag{10.10}$$

where the second equality results from the symmetry of the integrand. Next, we illustrate how to derive the density function $f_T(x)$ from equation (10.10) via the Fast Fourier Transform (FFT). FFT is an efficient algorithm for computing the following transformation of a vector $(\alpha_n,\ n = 1, \cdots, N-1)$ into a vector $(\beta_n,\ n = 1, \cdots, N-1)$, where N is typically a power of 2 :

$$\beta_n = \sum_{j=0}^{N-1} \exp\left(-\frac{2\pi i}{N} jn\right) \alpha_j\,.$$

This method is quicker than computing the discretization of the integral (10.10) since the FFT algorithm computes in only $O(n \log n)$ operations (rather than $O(n^2)$). The first step of the FFT consists in discretizing the integral (10.10). We denote Δz the step of discretization and N the number of steps. The discretization mesh is defined by

$$\{z_j\} = \{j\Delta z\ \in \mathbb{R}^+ \,|\, 0 \le j \le N-1\}\,.$$

We then need to define a mesh of discretization for the density values $f_T(x)$, spaced by Δx and counting the same number N of elements as $\{z_j\}$. The mesh of the density is then

$$\{x_n\} = \{-x_{min} + n\Delta x\ \in \mathbb{R}^+ \,|\, 0 \le n \le N-1\}\,,$$

where $x_{min} = \frac{N\Delta x}{2}$ and with the following condition on the steps of discretizations $\Delta z \Delta x = \frac{2\pi}{N}$. Therefore, we can reformulate (10.10) into the following form

$$
\begin{aligned}
& f_T(x_n) = \frac{1}{\pi} \int_0^{+\infty} \Phi_X(T,z)\, e^{-izx_n} dz \\
\iff \qquad & f_T(x_n) = \frac{1}{\pi} \sum_{j=0}^{N-1} \Phi_X(T,z_j)\, e^{-iz_j x_n}\, \Delta z \\
\iff \qquad & \underbrace{\pi\, f_T(x_n)}_{\beta_n} = \sum_{j=0}^{N-1} e^{-i\frac{2\pi}{N} j\, n}\, \underbrace{e^{i\, z_j\, x_{min}}\, \Phi_X(T,z_j)\Delta z}_{\alpha_j} . \qquad (10.11)
\end{aligned}
$$

This way we can apply the FFT with $\alpha_j = e^{i\, z_j\, x_{min}}\, \Phi_X(T,z_j)\Delta z$ in order to obtain the output vector $\beta_n = \pi\, f_T(x_n)$ for $n \in 0, \cdots, N-1$. Finally, once we estimated the density via the FFT, we can easily derive the ε-quantile of X_T denoted x_ε. Using equation (7.1), we find that the VaR level q of the portfolio value V_T at maturity is equal to

$$q = e^{x_\varepsilon} + F_T\,. \qquad (10.12)$$

The TVaR tv at level ε of V_T can then be computed by discretizing (7.4) :

$$tv = \frac{1}{\varepsilon} \sum_{x_n :\, x_n \le \log(q - F_0 e^{rT})} e^{x_n} f_T(x_n) \Delta x \;+\; F_0 e^{rT}\,. \qquad (10.13)$$

Availability of data and material

The datasets and code generated during and/or analyzed during the current study are available from the corresponding author on reasonable request.

Acknowledgments

This work was supported by the FNRS, Belgium under Grant no. 33658713.

References

E. Abi Jaber (2019) Lifting the heston model, *Quantitative Finance* **19** (12), 1995–2013.

E. Abi Jaber, M. Larsson, S. Pulido *et al.* (2019) Affine volterra processes, *Annals of Applied Probability* **29** (5), 3155–3200.

J. Ackermann, T. Kruse & L. Overbeck (2020) Inhomogeneous affine volterra processes, *arXiv preprint arXiv:2012.10966* .

C. Andrieu, A. Doucet & R. Holenstein (2010) Particle markov chain monte carlo methods, *Journal of the Royal Statistical Society: Series B (Statistical Methodology)* **72** (3), 269–342.

P. Artzner, F. Delbaen, J.-M. Eber & D. Heath (1999) Coherent measures of risk, *Mathematical finance* **9** (3), 203–228.

S. Balder, M. Brandl & A. Mahayni (2009) Effectiveness of cppi strategies under discrete-time trading, *Journal of Economic Dynamics and Control* **33** (1), 204–220.

M. Bennedsen, A. Lunde & M. S. Pakkanen (2016) Decoupling the short-and long-term behavior of stochastic volatility, *arXiv preprint arXiv:1610.00332* .

M. Bennedsen, A. Lunde & M. S. Pakkanen (2017) Hybrid scheme for brownian semistationary processes, *Finance and Stochastics* **21** (4), 931–965.

F. E. Benth, A. Khedher & M. Vanmaele (2020) Pricing of commodity derivatives on processes with memory, *Risks* **8** (1), 8.

L. Bergomi & J. Guyon (2012) Stochastic volatility's orderly smiles, *Risk* **25** (5), 60.

P. Bertrand & J.-L. Prigent (2001) Portfolio insurance strategies: Obpi versus cppi. In: *Conférence Internationale en Finance*.

P. Bertrand & J.-L. Prigent (2016) Portfolio insurance: The extreme value approach applied to the cppi method, *Extreme Events in Finance: A Handbook of Extreme Value Theory and Its Applications* **465**.

P. Bertrand & J.-L. Prigent (2019) On the optimality of path-dependent structured funds: The cost of standardization, *European Journal of Operational Research* **277** (1), 333–350.

F. Black & R. Jones (1987) Simplifying portfolio insurance, *Journal of portfolio management* **14** (1), 48.

N. Branger, A. Mahayni & J. C. Schneider (2010) On the optimal design of insurance contracts with guarantees, *Insurance: Mathematics and Economics* **46** (3), 485–492.

M. Cadoni, R. Melis & A. Trudda (2017) Pension funds rules: Paradoxes in risk control, *Finance Research Letters* **22**, 20–29.

G. M. Caporale, L. Gil-Alana & A. Plastun (2018) Is market fear persistent? a long-memory analysis, *Finance Research Letters* **27**, 140–147.

R. Cont & P. Tankov (2009) Constant proportion portfolio insurance in the presence of jumps in asset prices, *Mathematical Finance: An International Journal of Mathematics, Statistics and Financial Economics* **19** (3), 379–401.

K. Diethelm, N. J. Ford & A. D. Freed (2002) A predictor-corrector approach for the numerical solution of fractional differential equations, *Nonlinear Dynamics* **29** (1), 3–22.

A. Doucet, N. De Freitas & N. Gordon (2001) An introduction to sequential monte carlo methods. In: *Sequential Monte Carlo methods in practice*, 3–14. Springer.

J.-L. Dupret, J. Barbarin & D. Hainaut (2021) Impact of rough stochastic volatility models on long-term life insurance pricing, Tech. rep.

O. El Euch, J. Gatheral & M. Rosenbaum (2019) Roughening heston, *Risk* , 84–89.

O. El Euch & M. Rosenbaum (2019) The characteristic function of rough heston models, *Mathematical Finance* **29** (1), 3–38.

O. El Euch, M. Rosenbaum *et al.* (2018) Perfect hedging in rough heston models, *Annals of Applied Probability* **28** (6), 3813–3856.

J. Gatheral (2011) *The volatility surface: a practitioner's guide*. John Wiley & Sons.

J. Gatheral, T. Jaisson & M. Rosenbaum (2018) Volatility is rough, *Quantitative Finance* **18** (6), 933–949.

J. Gatheral & M. Keller-Ressel (2019) Affine forward variance models, *Finance and Stochastics* **23** (3), 501–533.

S. J. Grossman & J.-L. Vila (1992) Optimal dynamic trading with leverage constraints, *Journal of Financial and Quantitative Analysis* , 151–168.

D. Hainaut (2011) Risk management of cppi funds in switching regime markets, *Bankers, Markets and Investors. August* .

M. Johannes & N. Polson (2010) Mcmc methods for continuous-time financial econometrics. In: *Handbook of Financial Econometrics: Applications*, 1–72. Elsevier.

M. Keller-Ressel, M. Larsson & S. Pulido (2018) Affine rough models, *arXiv preprint arXiv:1812.08486* .

G. Kingston (1989) Theoretical foundations of constant-proportion portfolio insurance, *Economics Letters* **29** (4), 345–347.

R. Lord, R. Koekkoek & D. V. Dijk (2010) A comparison of biased simulation schemes for

stochastic volatility models, *Quantitative Finance* **10** (2), 177–194.

S. Momani & N. Shawagfeh (2006) Decomposition method for solving fractional riccati differential equations, *Applied Mathematics and Computation* **182** (2), 1083–1092.

D. Pain & J. Rand (2008) Recent developments in portfolio insurance, *Recent Developments in Portfolio Insurance* .

L. Paulot & X. Lacroze (2009) Efficient pricing of cppi using markov operators, *Available at SSRN 1326297* .

A. F. Perold & W. F. Sharpe (1988) Dynamic strategies for asset allocation, *Financial Analysts Journal* **44** (1), 16–27.

J.-L. Prigent & P. Bertrand (2003) Portfolio insurance strategies: a comparison of standard methods when the volatility of the stock is stochastic, *Available at SSRN 450061* .